

Ultrafast extreme ultraviolet holography: dynamic monitoring of surface deformation

Ra'anan I. Tobey, Mark E. Siemens, Oren Cohen, Margaret M. Murnane, and Henry C. Kapteyn

Department of Physics and JILA, University of Colorado and NIST, and NSF Engineering Research Center in Extreme Ultraviolet Science and Technology, Boulder, Colorado 80309-0440, USA

Keith A. Nelson

Department of Chemistry, Massachusetts Institute of Technology, Cambridge, Massachusetts 02139, USA

Received August 29, 2006; revised October 13, 2006; accepted October 24, 2006;
posted October 31, 2006 (Doc. ID 74469); published January 12, 2007

We demonstrate femtosecond time-resolved dynamic Gabor holography using highly coherent extreme ultraviolet light generated by high harmonic upconversion of a femtosecond laser. By reflecting this light from an impulsively heated surface, we implement a simple and robust single-reflection geometry for phase-sensitive holographic detection at extreme UV wavelengths. Using this setup, we study the ultrafast deformation and subsequent acoustic oscillations within a thin metal film. These measurements exhibit subpicometer spatial sensitivity in the vertical dimension. © 2007 Optical Society of America

OCIS codes: 190.4870, 240.6490, 240.0310, 320.7110.

Time-resolved interferometric imaging techniques have attracted attention recently because of their ability to precisely monitor dynamic changes in both space and time.^{1–3} These experiments make use of a pump–probe geometry, where an optical pump distorts the sample, while a time-delayed probe captures the induced dynamics. Experiments are performed by placing the sample in one arm of an interferometer. In some experiments,^{1,2} a dynamic interference pattern is then captured on a CCD camera, and a reconstruction algorithm is used to obtain the sample evolution. This technique was used to study femtosecond dynamics of electrons at metal surfaces and in semiconductors with lateral spatial resolutions approaching 1 μm and with phase sensitivities of $\lambda/1000$ at 800 nm. Also, interferometric detection has been employed to study surface deformation on ultrafast time scales³ with phase resolutions of the order of 1 pm ($\lambda/1,000,000$).

The use of extreme ultraviolet (EUV) radiation for interferometric detection offers the potential for simultaneous subangstrom displacement sensitivity and increased lateral spatial resolution due to the shorter probe wavelength. However, interferometric measurements with EUV light are difficult because EUV beam splitters are not well developed and EUV components have poor reflectivity. Typical sample reflectivities are around 1%, making a Michelson interferometer impractical. Nevertheless, a few experiments to date have employed interferometric detection with EUV light on relatively long time scales and large spatial dimensions. For example, the electron density profile of laser-produced plasmas can be measured using EUV interferometry⁴ because the high frequency of the EUV light is above the plasma frequency of the expanding plasma. Other interferometric experiments have directly measured the complex index of refraction of some materials at EUV wavelengths.⁵ However, to date experiments have not explored EUV interferometry or holography

with simultaneously high spatial and temporal resolution.

In this Letter we extend previous work in our group, which implemented static Gabor holography,⁶ to study the dynamics of optically generated bulk longitudinal acoustic wave packets in a thin metal film with simultaneously high temporal and longitudinal (vertical) resolution in the vertical dimension. A femtosecond near-infrared laser pulse is used to launch the acoustic waves. A fully coherent EUV beam⁶ probes the subsequent acoustic oscillations at the surface of the thin film. We use a novel excitation geometry where a narrow line on the sample is excited by the infrared-pump laser, which is then probed by a much larger EUV beam. The unperturbed sample reflects the EUV (reference) beam, while the pumped region diffracts the object beam to form a dynamic hologram. This is a simple, robust, single-reflection geometry for studying transient dynamics with femtosecond time resolution. We demonstrate subpicometer sensitivity to surface displacements, and we find that EUV probing of surface deformation is largely free of ambiguity associated with electronic dynamics. This property will prove important for investigating surface deformation immediately after impulsive heating—a regime in which the surface deformation signal is generally screened by the electronic signal if probed by visible wavelengths.⁷

The experimental geometry is shown in Fig. 1. Light from a titanium-doped sapphire laser-amplifier system^{8,9} operating at a repetition rate of 2 kHz, with a 30 fs pulse duration, is split into pump and probe beams. Light in the probe arm is upconverted into the EUV using the process of high harmonic generation in an argon-filled hollow waveguide.¹⁰ The waveguide allows the conversion process to be well phase matched over an extended propagation length, leading to the generation of a fully coherent EUV output beam.⁶ The EUV pulses generated in this manner yield a spectrum of ~ 5 (odd) harmonic orders, peaked

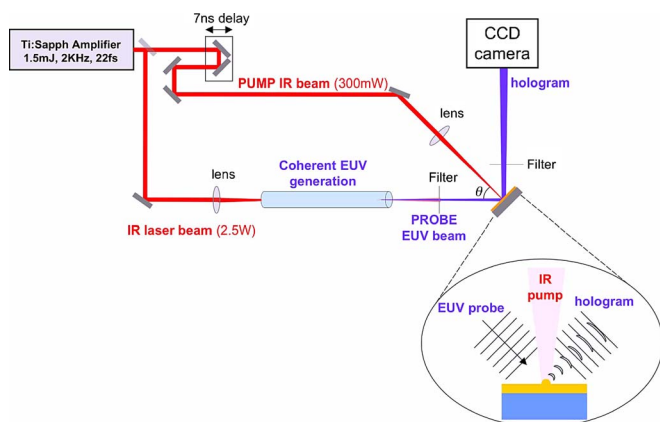


Fig. 1. Experimental setup for excitation and holographic detection of surface deformation. The femtosecond pump pulse excites a line focus on the thin film nickel sample. The EUV beam probes a larger region of the sample than the pump. Unperturbed regions of the sample reflect the reference beam, which interferes with the diffracted EUV light from the perturbed regions for holographic detection.

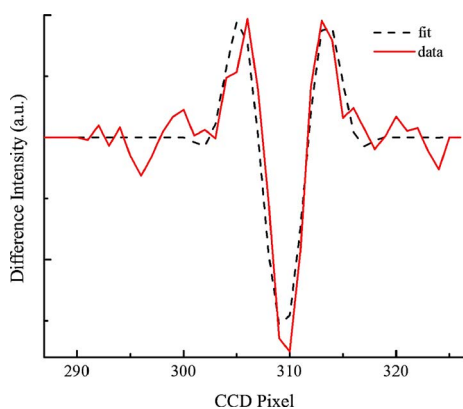


Fig. 2. Difference in reflected EUV intensity from a $2\ \mu\text{m}$ thick aluminum film, with and without the pump pulse present, at a time delay of 150 ps. The solid line shows the dynamic hologram exhibiting the characteristic far field diffraction pattern of a slit. The calculated signal is shown as a dashed line. By analyzing many such images as a function of time delay, the diffraction pattern can be seen to disappear and reappear, as a bulk longitudinal acoustic wave packet propagates into the bulk and undergoes multiple reflections at the film/substrate interface.

at the 27th harmonic order with a wavelength of 29 nm. The EUV light then passes through three freestanding thin aluminum filters (600 nm total) to eliminate the residual laser light exiting the fiber while transmitting approximately 1% of the EUV radiation. The pump beam is sent into a computer-controlled delay line. A single cylindrical lens is used to generate a $1.5\ \text{cm} \times 77\ \mu\text{m}$ line focus on the sample. Experiments are performed on thin metal films that were thermally evaporated onto fused silica substrates. The probe spot is $\sim 1\ \text{mm}$ in diameter and spatially and temporally overlaps the pump beam on the sample surface, as shown in Fig. 1. In contrast with conventional pump-probe techniques, the excitation region of the sample resides wholly within the region being probed. This geometry allows the EUV reflection from the unperturbed region of the sample to serve as the reference beam for holo-

graphic detection. When the sample is perturbed by the line-focus pump excitation, the EUV intensity pattern on the camera corresponds to the interference of light reflected from the flat surfaces of the sample and light diffracted from the dynamically varying, line-pumped region. We observe a dynamically changing single-slit diffraction pattern that is shown in Fig. 2.

We obtain the width of the “slit” by calculating the hologram using a paraxial wave propagation simulation and fitting it to the experimental interference pattern (Fig. 2). Light reflecting from a pump-modulated surface experiences a change in the complex reflectivity coefficient $r(x)\exp[i\phi(x)]$, where $r(x)$ is the pump-induced change in reflectivity due to photoelastic and electronic effects, and $\phi(x)$ is the phase change from surface deformation.¹¹ However, as we will show below, our EUV probe is only sensitive to surface deformations. Assuming that the profile of the surface deformation is proportional to the Gaussian profile of the pump intensity, the pump-induced phase change at the surface is given by

$$\phi_F(x,t) = \frac{4\pi\Delta l_F(t)}{\lambda \cos(\theta)} \exp(-x^2/w^2), \quad (1)$$

where λ is the probing wavelength, $\Delta l_F(t)$ is the peak surface expansion dependent on the pump-probe delay time at a given pumping fluence, $\theta=45^\circ$ is the angle between the probe and the surface normal, and $w=77\ \mu\text{m}$ is the width of the pumped region. We note that the only free parameter in fitting the calculated to the experimental holograms is the peak surface expansion. Figure 2 shows one such fit, yielding $\Delta l = 0.022 \pm 0.003\ \text{nm}$. For our absorbed energy of $24\ \mu\text{J}$, we estimate that the peak temperature in the sample in this case is 600 K, which is well below the melting temperature. This temperature imposes an upper bound on the surface deformation of 0.1 nm, indicating that our measurement is reasonable. Differences between the signal and simulation in Fig. 2 are likely due to beam pointing instabilities in the laser system. Based on our fit results and a signal-to-noise ratio (SNR) of 35 (obtained from Fig. 3), we conclude that our sensitivity to surface deformation is 0.7 pm. This sensitivity is comparable to that obtained using the best visible interferometric techniques¹² and shows great promise for further improvements.

By analyzing the time evolution of a diffraction pattern such as that in Fig. 2, the transient thermoacoustic dynamics can be extracted. Data are accumulated by averaging 25–75 CCD exposures, where each exposure is 20–100 ms (40–200 laser pulses) long. Scans showing good SNRs, as shown in Fig. 3, take about 1 h. A single data point comprises the difference between CCD images taken with and without excitation of the sample. Figure 3 plots the surface deformation as a function of time delay between the pump and probe for an 80 nm nickel film on fused silica. Immediately after time zero, there is a sharp increase in signal with a rise time of $\tau_{20-80} = 2\ \text{ps}$. This initial rise is due to thermal expansion of the sample surface after impulsive excitation. The laser-induced

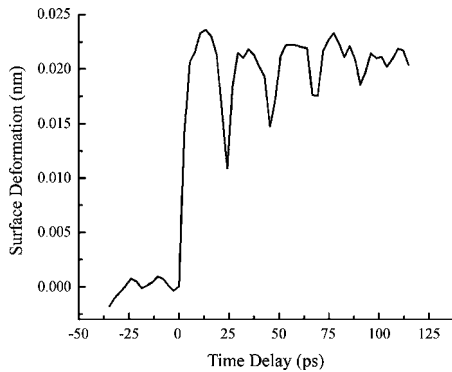


Fig. 3. Temporal evolution of a holographic signal such as shown in Fig. 2, measuring both the initial thermal expansion of the surface and the repeated arrival of an acoustic wave packet at the probed surface. An oscillation frequency of ≈ 46 GHz is commensurate with a 66 nm nickel film, which is in reasonable agreement with the nominal thickness of 80 ± 20 nm.

thermal stress near the surface relaxes by launching a broadband longitudinally polarized strain pulse into the metal film. This acoustic wave packet then propagates through the thin film sample until it reaches the film–substrate interface, where a portion of the wave packet is reflected back towards the sample surface. The arrival of the wave packet at the probed surface is marked by an additional modulation of the surface and the resulting holographic signal. Partial reflection of the acoustic wave packet at the free surface leads to successive echoes as the wave packet bounces between the two interfaces. By Fourier transforming the temporal evolution of the diffraction pattern, such as that shown in Fig. 3, an oscillatory surface deformation due to multiple reflection of the acoustic wave packet can be extracted at a frequency of 45.7 ± 1.1 GHz. Using tabulated values for the longitudinal acoustic velocity in nickel ($v_1 = 6040$ m/s), we retrieve a film thickness of 66.1 ± 1.6 nm. This value is in qualitative agreement with the nominal film thickness of 80 ± 20 nm measured by a crystal microbalance during the thin film evaporation process.

Of particular interest in Fig. 3 is the absence of signal arising from fast electron dynamics at time zero, in contrast with acoustic measurements on Ni using an optical probe.¹³ This is because small pump-induced changes in electronic density at the Fermi edge significantly change the refractive index at visible wavelengths, but have little effect in the EUV. Furthermore, the probe light field does not couple to the lattice distortions caused by the thermal density change and the subsequent propagating wave packet. A temperature increase of 300 K results in a maximum density decrease of 0.9%, which in turn affects the index of refraction. At EUV wavelengths, the index of refraction can be written as $n = (1 - \delta) - i\beta$, where δ and β are proportional to the density.¹⁴ Using the Fresnel equations we calculate a density-induced change in reflectivity of 0.0006, which is 20 times lower than the change in reflectivity for an optical probe. According to our model, the holographic signal from EUV reflectivity change is $50\times$ weaker

than the signal due to surface deformation. Additionally, the shape of the acoustic pulses in Fig. 3 matches those in an experiment on Ni by Saito *et al.*,¹³ in which they modeled and observed a signal dominated by surface modulation. The fact that this straightforward method of EUV probing of surface deformation is largely free of ambiguities associated with electronic and photoelastic effects is an important advantage over previous photoacoustic measurement techniques.

In summary, we have demonstrated a simple and robust holographic geometry for dynamic, phase-sensitive detection of surface deformation using EUV radiation. These experiments extend the scope of previously demonstrated Gabor holography to the study of transient acoustic dynamics. With phase sensitivities of better than $\lambda/43,000$ at 30 nm, we detect ultrafast surface deformations and subsequent acoustic echoes in thin metal films. We anticipate extending phase-sensitive detection to study other transient dynamics, such as thermal transport in nanostructures with spatial dimensions on order of 100 nm. This is smaller than the phonon mean free path in many materials and is too small to be probed optically.

This work was supported by the Chemical Sciences, Geosciences, and Biosciences Division of the Office of Basic Energy Sciences, U.S. Department of Energy. This research made use of facilities supported by the NSF Engineering Research Center in EUV Science and Technology. R. I. Tobey's e-mail address is Ra.Tobey@colorado.edu.

References

1. V. V. Temnov, K. Sokolowski-Tinten, P. Zhou, and D. von der Linde, *Appl. Phys. A* **78**, 483 (2004).
2. D. J. Funk, D. S. Moore, S. D. McGrane, J. H. Reho, and R. L. Rabie, *Appl. Phys. A* **81**, 295 (2005).
3. D. H. Hurley and O. B. Wright, *Opt. Lett.* **24**, 1305 (1999).
4. J. Filevich, J. J. Rocca, M. C. Marconi, R. F. Smith, J. Dunn, R. Keenan, J. R. Hunter, S. J. Moon, J. Nilsen, A. Ng, and V. N. Shlyaptsev, *Appl. Opt.* **43**, 3938 (2004).
5. C. Chang, E. Anderson, P. Naulleau, E. Gullikson, K. Goldberg, and D. Attwood, *Opt. Lett.* **27**, 1028 (2002).
6. R. A. Bartels, A. Paul, H. Green, H. C. Kapteyn, M. M. Murnane, S. Backus, I. P. Christov, Y. W. Liu, D. T. Attwood, and C. Jacobsen, *Science* **297**, 376 (2002).
7. G. L. Eesley, *Phys. Rev. B* **33**, 2144 (1986).
8. M. Asaki, C. P. Huang, D. Garvey, J. Zhou, H. C. Kapteyn, and M. M. Murnane, *Opt. Lett.* **18**, 977 (1993).
9. S. Backus, R. Bartels, S. Thompson, R. Dollinger, H. C. Kapteyn, and M. M. Murnane, *Opt. Lett.* **26**, 465 (2001).
10. A. Rundquist, C. Durfee, Z. Chang, C. Herne, H. Kapteyn, and M. Murnane, *Science* **280**, 1412 (1998).
11. O. B. Wright and K. Kawashima, *Phys. Rev. Lett.* **69**, 1668 (1992).
12. C. J. K. Richardson, M. J. Ehrlich, and J. W. Wagner, *J. Opt. Soc. Am. B* **16**, 1007 (1999).
13. T. Saito, O. Matsuda, and O. B. Wright, *Phys. Rev. B* **67**, 205421 (2003).
14. D. Attwood, *Soft X-Rays and Extreme Ultraviolet Radiation: Principles and Applications* (Cambridge U. Press, 1999).